Journal of Chromatography, 593 (1992) 339–355
Elsevier Science Publishers B.V., Amsterdam

CHROMSYMP. 2437

Asymmetric-channel flow field-flow fractionation with exponential force-field programming

J. J. Kirkland*, C. H. Dilks, Jr., S. W. Rementer and W. W. Yau

E. I. DuPont de Nemours Co., Experimental Station, P.O. Box 80228, Wilmington, DE 19880-0228 (USA)

ABSTRACT

Equipment and techniques have been developed to program the crossed-flow force fields with parallel-plate, asymmetric channels in flow field-flow fractionation (FlFFF). Force-field programming permits the rapid separation of samples with a wide range of molecular sizes; resolution is easily varied. Detectability of late-eluting components is enhanced as a result of band sharpening. Force-field programming probably can be performed with many functions. Exponential force-field decay method produces retention times *vs.* diffusion coefficient or particle size plots that are more linear than those from a constant force field. Resolution and measurement precision is more constant over the separation range. The exponential function also simplifies computer software measuring diffusion-coefficient and particle-size distributions. Optimum operating parameters for a desired FlFFF separation are predicted with a quantitative exponential force-field decay theory. Force-field programming significantly enhances the utility of the mild FlFFF method. Appropriate samples for this method include synthetic and natural polymers, organic and inorganic colloids and a variety of particulates.

INTRODUCTION

Flow field-flow fractionation (FlFFF) is one of a family of field-flow fractionation (FFF) methods that exhibit unique properties for separating and characterizing a wide variety of macromolecular samples [1–5]. However, FlFFF is proving to be one of the most versatile and generally applicable of all of the FFF methods. FlFFF is capable of separating smaller macromolecules such as $\geqslant 10^4$ molecular weight proteins [6,7], but also is well suited for describing the size of a wide range of colloidal particulates [4,7–9]. Retention in FlFFF is based on physical first principles [8]. Fundamental information such as diffusion coefficients is available from FlFFF retention data, and purified components are easily isolated during separations. FlFFF competes with sedimentation FFF (SdFFF) for many potential applications [4,5], but SdFFF equipment is more complicated and expensive, and compounds with molecular weights less than about $2 \cdot 10^5$ are not retained with the highest force fields yet reported for this method [10].

In FlFFF, the force field needed for the separation is generated by flowing a carrier liquid across the channel thickness by means of semi-porous membranes forming the walls of the thin separating channel. FlFFF separations have been successfully carried out in channels made with parallel plates using two semi-permeable membranes [4,11] or in a porous hollow fiber [12]. However, the most successful FlFFF separations to date have been performed with the so-called asymmetric channel [6,7,13,14]. This approach uses only a single semi-permeable membrane at the channel bottom as the accumulation wall. A solid plate at the top forms the upper wall of the channel. To date most FlFFF separations with asymmetric channels have been conducted with constant force fields, that is, a constant volumetric flow of liquid carrier across the channel through the single semi-porous membrane. Equipment for this form of FlFFF is relatively inexpensive, and a simple theory describes sample properties as a function of observed retention [6]. FlFFF can be conveniently performed using constant force fields if sample components do not span too large a range in

molecular sizes (typically < 50-fold). The highest resolution of closely eluting components is generally obtained with this approach.

However, as with the other FFF methods, the use of constant force fields limits the range of useful elution of components in a single separation [11]. In constant force-field separations, the resolution varies during the separation; the resolution of components increases with increasing retention. Detection is also difficult for highly retained materials owing to inherent broadening of bands with increasing retention. In theory, programming the flow eluting from the channel minimizes some of these limitations. Unfortunately, however, this approach has serious practical problems. Changes in the channel effluent flow cause significant difficulties in maintaining constant baselines and detector response for quantification.

To reduce the limitations of constant force-field operation in FlFFF, Wahlund *et al.* [11] programmed the force field during separations of water-soluble polymers using a rectangular channel with two semi-permeable membranes. The most successful programming used by these workers involved exponential decay of the force field. This is the programming form previously used extensively by Kirkland and co-workers for both sedimentation [15–17] and thermal [18,19] FFF separations. Other forms of continuous force-field programming undoubtedly also can be used advantageously in FlFFF. It is often convenient to field program the initial separation of an unknown sample to include a possible broad range of molecular sizes. This preliminary run is then followed by runs under constant field to focus on a desired narrower size range.

This paper describes the theory, equipment and technique for programming the force field exponentially within the channel during separation using asymmetric FlFFF channels. Although more complicated equipment is required for automation, this approach eliminates many of the limitations of the constant force-field method. Quantitative theory and software have been developed to describe elution when the force field is exponentially decayed during the separation. This combination permits the convenient measurement of diffusion-constant and particle-size distributions of macromolecules and particulates. Exponential decay of the force field during the separation results in more uniform resolution of components across the elution profile. With a programmed force field, bands for highly retained components are compressed, making detection and quantitative measurement easier. Finally, the described method permits a constant flow through the detector during the separation, facilitating good detector baselines and subsequent quantitative measurements.

EXPERIMENTAL

FlFFF apparatus

Fig. 1 shows the general arrangements of components in our FlFFF equipment. Solvent metering devices 1–3 were Model 870 reciprocating pumps (DuPont Instruments, Wilmington, DE, USA). Pump 4 was a Model LC-5000 syringe pump (Isco, Lincoln, NE, USA). This pump was modified electrically to permit it to be used as an "unpump" to meter out precisely the channel effluent during the separation. This arrangement allows a constant flow out of the channel and through the detector. Flows from these systems were monitored by collecting pumped mobile phase in a volumetric flask for an observed time period. Model EC3W electronically actuated valves (Valco Instruments, Houston, TX, USA) were used as "on–off" and "focus–detector" valves. A Model EC6W electronically actuated valve (Valco Instruments) was the sample injector. All of these units were controlled with in-house-developed Turbo-Pascal software used on a PS-2 Model 30-286 personal computer (IBM, Boca Raton, FL, USA).

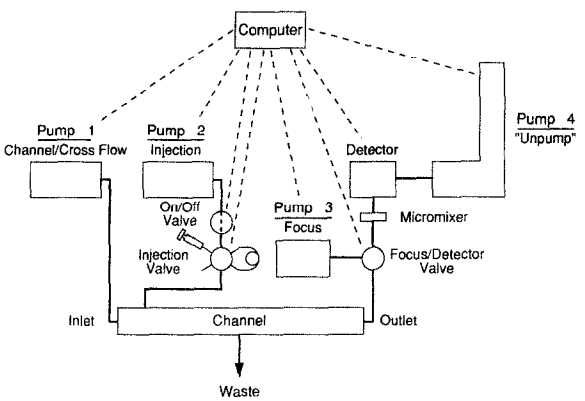

Fig. 1. Schematic diagram of FlFFF apparatus for cross-flow programming.

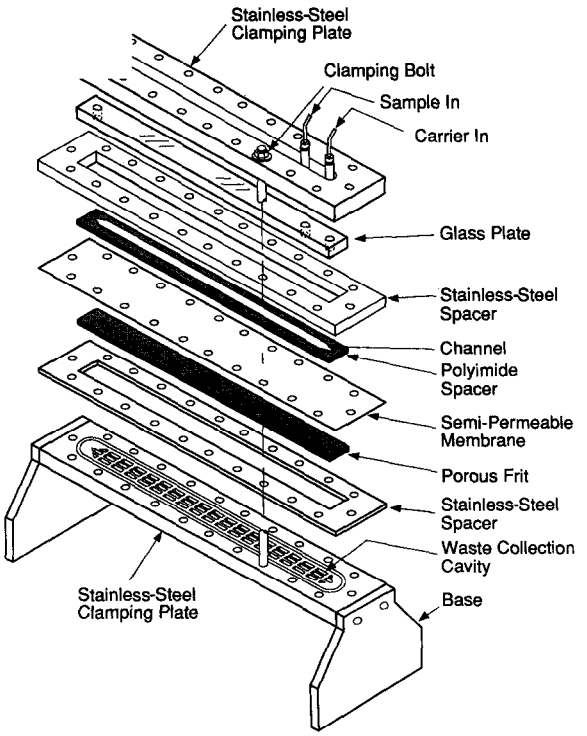

Fig. 2. Asymmetric FlFFF channel assembly: exploded view.

The micromixer was a 0.25-ml magnetically stirred stainless-steel chamber. Detection was with a Model 783 UV–visible spectrophotometric high-performance liquid chromatographic detector (Kratos Analytical, Ramsey, NJ, USA). Detector output was displayed on a Model 822B10-3 recorder (Esterline-Angus Instrument, Indianapolis, IN, USA).

The FlFFF channel assembly is depicted by the exploded view in Fig. 2. Fig. 3 shows a scaled end-view of the channel assembly. The channel was of the rectangular asymmetric configuration [6], as depicted in Fig. 4. The separating channel was 41.0 × 2.0 cm, formed with a nominal 0.025-cm thick Mylar polyester or Kapton polyimide film spacer (DuPont, Wilmington, DE, USA). The actual channel thickness was measured as 0.0241 cm by injecting a small sample of cytochrome *c* with no force field several times, and noting the average first moment of the eluted peak at a flow-rate of 0.20 ml/min (corrections were made for the extra-channel volume leading to the detector). As the volume, length and width of the channel were known, the thickness could be calculated. This channel was formed with 90° triangular inlet and outlet configurations.

The semi-permeable channel accumulation wall was a YM10 Diaflo ultrafiltration membrane (Amicon, Danvers, MA, USA). This membrane was

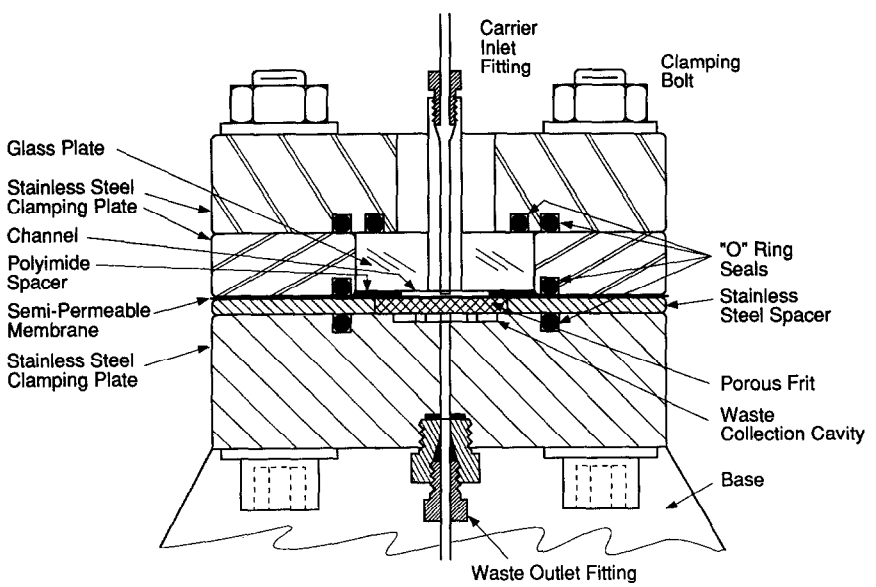

Fig. 3. Asymmetric FlFFF channel assembly: end-view.

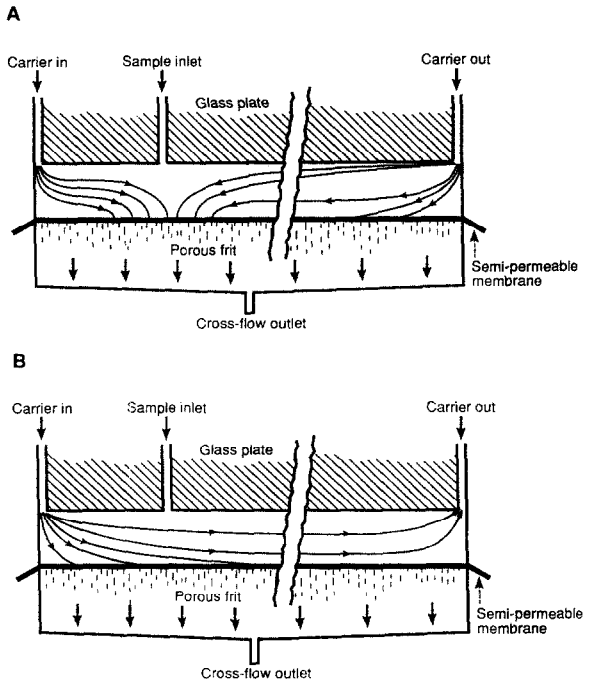

Fig. 4. Asymmetric channel for FlFFF. (A) Sample injection, relaxation and focusing step; (B) elution step.

supported by a precision-grade, 1/8-in. thick, 5-μm porous polyethylene frit (General Polymer, West Reading, PA, USA). Buna-N O-rings (Mercer Rubber, Philadelphia, PA, USA) were used to seal the channel to the supporting plates. A drilled float-glass plate (Kaufman Glass, Wilmington, DE, USA) was the upper wall of the asymmetric channel. Sample injection was carried out through an injection port that was 3.5 cm downstream from the liquid carrier inlet port, in a manner similar to that described by Wahlund and Litzen [7]. The various units of the channel assembly were fabricated at the DuPont Experimental Station.

Operation of the FlFFF apparatus in the force-field programmed mode typically proceeds as follows (see Fig. 1). Simultaneously using pump 1 and "unpump" 4, the channel is first conditioned with the mobile phase carrier until a constant detector baseline is obtained. Pump 4 is then isolated with the "focus–detector" valve. The sample is slowly injected into the channel with mobile phase carrier by actuating pump 2 and displacing the sample from the loop of the injector valve (usually at 0.06–0.1 ml/min for a volume about twice the total volume of the sample loop and the connecting line). Simultaneously during this injection period, pumps 1 and 3 are actuated at flow-rates appropriate to focus the sample in a narrow band just below the sample inlet. This focusing approach is similar to that developed by Wahlund *et al.* [6,7,14]. Following the injection–focusing period, the "on–off" valve is closed. Sample focusing–relaxation can be continued with flow from pumps 1 and 3, if desired, or, if sufficient focusing–relaxation has been accomplished during injection, the "focus–detector" valve is actuated to close off pump 3 and access the "unpump" 4. Appropriate flow metering is then set on pumps 1 and 4 to conduct the desired separation. All steps in this procedure are conducted by the computer. The operator specifies the operating procedure by completing a software parameter block prior to the desired separation. The sample loop is filled manually, and the operator actuates the computer program to conduct the experiment automatically.

Separation data were collected on a PE/Nelson ACCESS·CHROM data-handling system (Nelson Analytical, Cupertino, CA, USA). In-house-developed software for the diffusion-coefficient or particle-size calculations and outputs was in FORTRAN 77 on a Vax 3100 computer (Digital Equipment, Maynard, MA, USA).

Reagents and chemicals

The proteins, Col E1 amp plasmid DNA, and Tris buffer were obtained from Sigma (St. Louis, MO, USA). Plasmid pSP 65 DNA was from Boehringer Mannheim Biochemicals (Indianapolis, IN, USA). Silica sol samples were prepared within DuPont. Samples of *Streptococcus faecalis* bacteria were kindly supplied by R. C. Ebersole of DuPont. Other materials for buffers and mobile phase additives were from J. T. Baker (Phillipsburg, NJ, USA).

THEORY

Retention with constant force field

Retention in FlFFF separations with a rectangular asymmetric channel and a constant force field (cross-flow) has previously been described by Wahlund and Giddings [6]. Retention times for well-retained components in such a system are described by

$$t_R = \left(\frac{W^2}{6D}\right) \ln \left[\frac{\frac{z}{L} - \left(\frac{V_c + V_{out}}{V_c}\right)}{\left(1 - \frac{V_c + V_{out}}{V_c}\right)} \right] \quad (1)$$

where t_R is the retention time of the component (s), W is the channel thickness (cm), D is the diffusion coefficient (cm^2/s), z is the sample focusing distance from the channel inlet (cm), L is the channel length (cm), V_c is the cross-flow flow-rate (ml/min) and V_{out} is the flow-rate out of the channel (ml/min). Hence, component diffusion coefficients can be directly calculated from the retention time if all operating parameters are known.

Using the well known Einstein diffusion equation [20], retention can be directly related to the size of comparable spherical particles. Therefore, particle sizes can be determined by measuring the retention time, according to

$$d_p = \frac{2RTt_R}{(W^2N\pi\eta) \ln \left[\frac{\frac{z}{L} - \frac{(V_c + V_{out})}{V_c}}{1 - \left(\frac{V_c + V_{out}}{V_c}\right)} \right]} \quad (2)$$

where d_p is the particle diameter (cm), R is the gas constant ($8.31 \cdot 10^7$ g $cm^2/s^2 \cdot K \cdot mol$), T is temperature (K), N is Avogadro's constant ($6.02217 \cdot 10^{23}$/mol) and η is the mobile phase viscosity (Poise; g/cm · s). With this expression, the size of particulates can be calculated directly from retention using known operating parameters.

The relationship between retention time and diffusion coefficient for a rectangular asymmetric channel and a constant force field can be depicted graphically as shown in Fig. 5. This log-linear plot was calculated from eqn. 1 using the arbitrary but typical operating parameters given. As noted above, important characteristics of constant force-field operation in FlFFF are illustrated in this plot. First, less than two decades of diffusion coefficients (or particle sizes) can be accessed in a single experiment with good precision and in a convenient time span. Second, the difference in retention for two components with the same relative difference in diffusion coefficient (or particle size) is non-linear. The difference in retention between two large particles with small diffusion coefficients is much greater than that for small particles with larger diffusion coefficients. This comparison is made for particle pairs having the same relative diffusion coefficient difference, related to the same percentage change, or the same spacing of the two diffusion coefficients on a logarithmic scale.

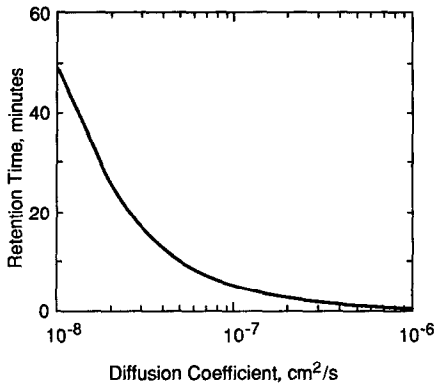

Fig. 5. Retention in FlFFF with asymmetric channel and constant force field. V_c = 1.0 ml/min; V_{out} = 0.5 ml/min; W = 0.0132 cm; L = 41.0 cm; z = 2.0 cm; breadth = 2.0 cm.

Retention using programmed force field with exponential decay

To remove some of the limitations of constant force-field FlFFF operation, we developed the apparatus described above to permit programmed force-field operation. This equipment can be used to create virtually any form of force-field program. What type of force-field programming would be optimum for convenient and accurate measurements in FlFFF? We found no clear theoretical basis that a particular function for programming the force field would create the best compromise for the desired conditions, mainly uniform resolution across a wide range of component sizes in a reasonable separation time. However, constant force-field data such in Fig. 5 produced retention *vs.* diffusion coefficient relationships that were suggestive of a logarithmic form. Previously, we had found that in both sedimentation [15–17] and thermal [18,19] FFF, exponential-decay of the force field results in a simple calibration: a plot of particle size or molecular weight *vs.* retention time produces a straight line. This format provides several practical advantages, including essentially uniform resolution (and uniform measurement precision) across the separa-

tion range and convenient quantification of data. Our previous success with exponential programming in sedimentation and thermal FFF and the preliminary results of Wahlund *et al.* [11] encouraged us to develop the theory and software for performing FlFFF with this force-field programming function for asymmetric rectangular channels.

Retention in FFF can be represented by the retention ratio, $R = V_o/V_R$, where V_o is the channel volume and V_R is the retention volume of the sample component. Components that are well retained can be represented by $R = 6\lambda$, where λ is the ratio of the mean height of the sample cloud from the accumulation wall to channel thickness [4]. Retention for well retained components in asymmetric rectangular channels using programmed force fields with exponential decay during the separation can be described by

$$t_R = \left[\frac{\tau}{\left(1 + \frac{6D\tau}{W^2}\right)}\right] \ln\left[1 + \left(\frac{L - z}{L}\right)\left(\frac{V_{co}}{V_{out}}\right)\left(1 + \frac{W^2}{6D\tau}\right)\right] \quad (3)$$

where τ is the time constant of the exponential decay (s) and V_{co} is the initial cross-flow flow rate (ml/min). Results can be expressed in terms of spherical particle size by using the Einstein relationship previously described for eqn. 2. Eqn. 3 is analogous to that described by Wahlund *et al.* [11] for rectangular channels with two semi-permeable membranes.

Previous studies in sedimentation [15–17] and thermal [18,19] FFF further demonstrated that a delay period equal to the time constant τ of the exponential decay added to the range of linearity for the molecular weight or particle size *vs.* retention time plot. This method also is useful in providing additional separation between early eluting peaks and the potentially interfering channel dead-volume peak. The usefulness of this approach suggested that this also should be investigated for FlFFF separations. We found that retention in rectangular asymmetric channels using programmed force field with exponential delay and decay can be described by

$$t_R = \tau + \left(\frac{\tau}{1 + \frac{6D\tau}{W^2}}\right) \ln\left\{1 + \left[\left(\frac{L - z}{L} \cdot \frac{V_{co}}{V_{out}}\right) \cdot \left(1 + \frac{W^2}{6D\tau}\right)\right] + \left[\frac{W^2}{6D\tau}\left(e^{\frac{-6D\tau}{W^2}} - 1\right)\right]\right\} \quad (4)$$

Derivations of eqns. 3 and 4 are given in the Appendix.

SOFTWARE FOR QUANTIFICATION

To quantify desired diffusion-coefficient and particle-size distribution measurements, it was necessary to solve eqn. 3 for the diffusion coefficient, D, (or the corresponding particle diameter, d_p) as a function of retention time, t_R. For this, an iterative numerical process was developed. This approach was simplified by combining certain parameters, so that

$$\alpha \equiv [(L - z)/L]\,[V_{co}/V_{out}] \quad (5)$$

and

$$S \equiv (6D\tau)/W^2 \quad (6)$$

Then, by iteration on S_i for the ith iteration,

$$S_i = \{\tau \ln[1 + \alpha(1 + 1/S_{i-1})]/t_R\} - 1 \quad (7)$$

This approach relates the diffusion coefficient, D, to the retention time, t_R, that is, $S = f(D)$. Initially,

$$1/S_o \equiv 0; \qquad S_1 = (\tau/t_R)\ln(1 + \alpha) - 1 \quad (8)$$

S_i is solved by iteration when S is large. For late-eluting particles, ΔS_j is calculated by

$$\Delta S_j = S(t_R + \Delta t_R) - S(t_R) \quad (9)$$

and

$$t_{R,j+1} = \tau/(1 + S_j + \Delta S_j)\ln\{1 + \alpha[1 + 1/(S_j + \Delta S_j)]\} \quad (10)$$

Here, ΔS_j is manipulated to achieve equal steps in t_R, which is defined by the sampling rate.

For retention near zero, S (being inversely related to t_R) is large and $1/S$ is small. For this case, the mathematical relationship $S = f(t_R, 1/S)$ is well behaved and eqn. 7 converges nicely, because the logarithmic term in eqn. 7 is dominated by $\ln(1 + \alpha)$. For later retentions, S is small and $1/S$ is large. The

logarithmic term in eqn. 7 is then dominated by $\ln(\alpha/S)$, and the iteration behaves poorly. Therefore, for later retentions, the S value for the previous retention slice j is used to estimate S_{j+1}, and the corresponding retention time is determined. The iteration searches for ΔS with eqn. 10 to achieve the known value of t_R. Fig. 6 is a graphical representation of ln S *vs.* retention time, t_R, for several values of the exponential-decay time constant τ.

RESULTS AND DISCUSSION

Effect of exponential-decay τ value on retention

The plots in Fig. 7 (based on eqns. 3 and 4) show the effect of changing the τ value on retention with asymmetric rectangular channels using exponentially programmed force fields. Plots are given for exponential programs devised with arbitrary but realistic operating parameters with and without delay prior to the force field programming. As expected, the delay increases the time of elution between the first peak and the channel dead volume peak. Smaller τ values result in plots that are increasingly more linear across the diffusion coefficient range selected for study. Larger τ values increase the non-linearity of the calibration. As noted previously, a linear calibration generally is advantageous. More uniform resolution and measurement precision occurs across the separation range of interest in a practical analysis time. Contrary to experiences in sedimentation and thermal FFF, imposing a delay before starting the exponential decay does not appear to improve the calibration linearity.

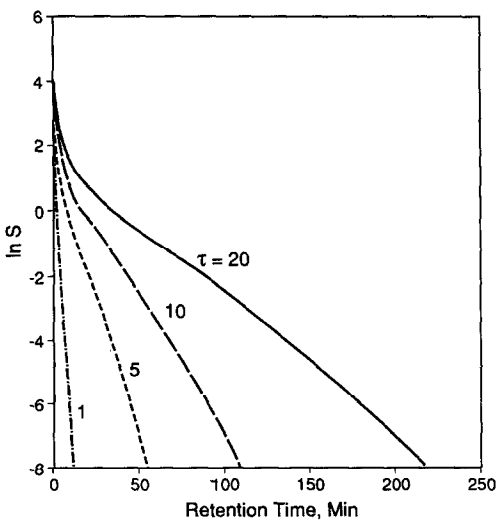

Fig. 6. Effect of combined retention parameters on retention time. See eqn. 10 for details.

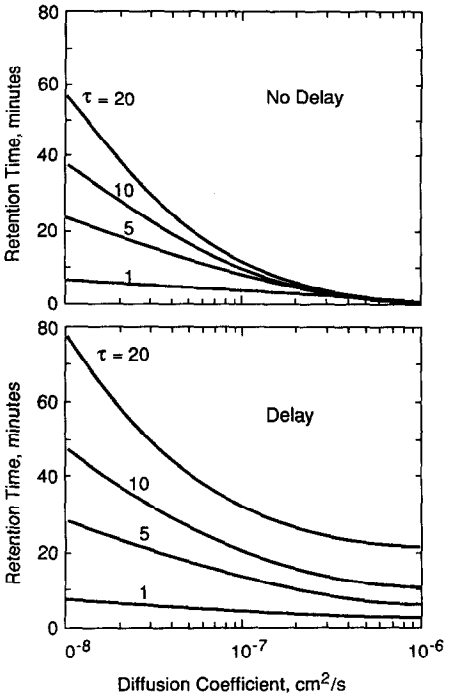

Fig. 7. Effect of τ value on retention in FlFFF with asymmetric channel using exponentially programmed force field. V_{co} = 9.5 ml/min; V_{out} = 0.5 ml/min; W = 0.0132 cm; L = 41.0 cm; z = 4.3 cm; breadth = 2.0 cm.

The results presented in Fig. 7 and the following simulated plots represent a rough first attempt to determine the effects of the various operating parameters for exponentially programming the force field in FlFFF for asymmetric channels. In these simulation plots, results at very low retention are less valid because of the assumption of $R = 6\lambda$ in eqns. 3 and 4. Still, these plots have been found useful in selecting useful experimental conditions for exponential programming in FlFFF.

As expected, similar effects were seen for retention time *vs.* particle diameter relationships, as shown in Fig. 8. In this instance, different operating parameters from those in Fig. 7 were selected to verify the general trends. Again, log-linear calibration and

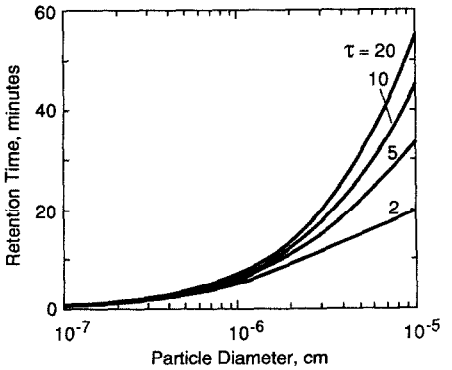

Fig. 8. Effect of τ value on particle retention in FlFFF with asymmetric channel using exponentially programmed force field. Conditions as in Fig. 7, except V_{out} = 1.0 ml/min.

approximately uniform separation are more nearly approached at smaller τ values. In this instance, calibration plots with delay in the force field before exponential decay were not prepared.

Effect of channel thickness on retention

The effect of channel thickness on retention with exponential force-field decay is shown in Fig. 9. These results suggest that log-linear calibration linearity is favored with wider channels, with channel thicknesses of 0.025 cm being about optimum for these particular operating conditions. No difference in calibration linearity is shown between separations carried out with and without delay before exponential decay. However, use of the delay does permit better separations of early-eluting peaks from the peak at the channel dead-time, t_o, at the expense of increased separation time. Note that increasing the channel thickness involves other compromises, as the separation time and band width also change [8]. Increasing the channel thickness does not appear to change significantly the relative separation between the same two components, as indicated by the approximately constant slope of the log-linear calibration graphs. The exception is very narrow channels and components with larger diffusion coefficients.

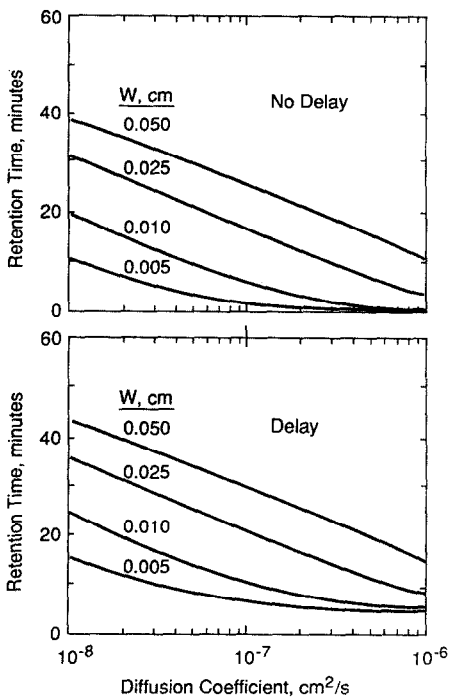

Fig. 9. Effect of channel thickness on retention in FlFFF with asymmetric channel using exponentially programmed force field. Conditions as in Fig. 7, except for W and τ = 5.0 min.

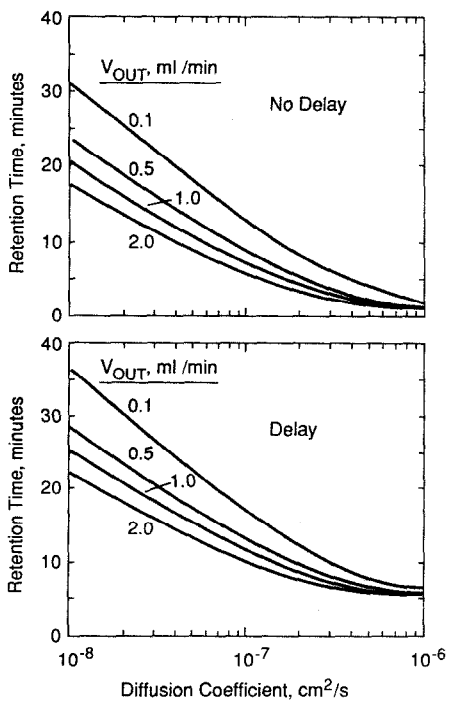

Fig. 10. Effect of channel effluent out-flow on retention in FlFFF with asymmetric channel using exponentially programmed force field. Conditions as in Fig. 7, except for V_{out} and τ = 5.0 min.

Effect of channel effluent out-flow on retention

Fig. 10 shows the effect of channel effluent out-flow V_{out} with an asymmetric rectangular channel on retention using exponential force-field programming. Calibration linearity is not seriously influenced by the level of V_{out}. However, larger retention time differences occur at lower flow-rates. Bands also should be narrower at lower flow-rates because of more favorable mass-transfer effects [8]. Again, imposing a delay before exponential decay does not affect calibration linearity.

Effect of initial cross-flow on retention

The effect of initial cross-flow, V_{co}, on retention in exponential force-field programming is shown in Fig. 11. As expected, increasing the initial force field increases retention. Calibration linearity also is better approached at higher initial force fields. Relative separations are not affected by the initial force field, except for small components with larger diffuslon coefficients. The possible deleterious effect of higher initial force fields causing problems with unwanted interaction of components with rough semi-permeable membranes forming the accumulation is not predicted by this analysis. The effect of possible steric interactions also is not featured.

Effect of channel length on retention

With a constant initial cross-flow, changes in channel length have little effect on retention in exponential programming, as shown in Fig. 12. These results suggest that shorter asymmetric channels (10–20 cm?) might be better suited for programmed separations in FIFFF under these conditions. This plot pictures components that are well retained on the channel until a certain lower force field is reached during programming. At that point components move rapidly down and out of the channel. The use of shorter channels may be practical because of the ability to focus the injected sample into a narrow band before starting the separation [7]. Focusing the injected sample mini-

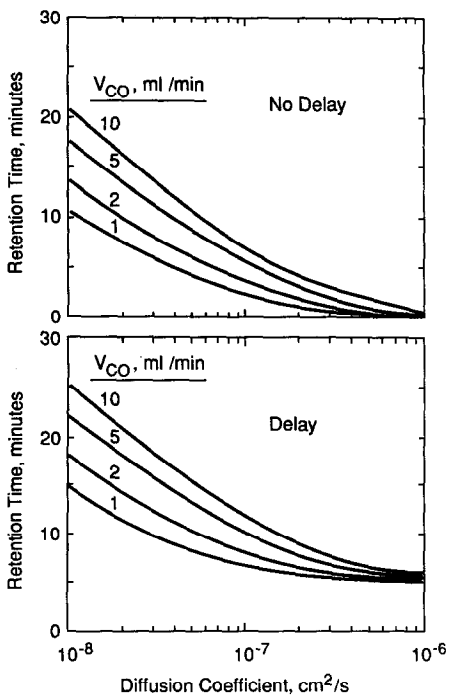

Fig. 11. Effect of initial cross-flow force field on retention in FIFFF with asymmetric channel using exponentially programmed force field. Conditions as in Fig. 7, except for V_{co} and τ = 5.0 min.

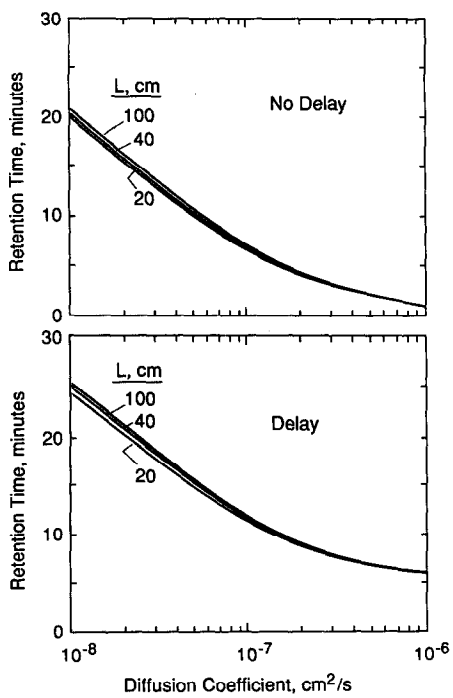

Fig. 12. Effect of channel length on retention in FIFFF with asymmetric channel using exponentially programmed force field: constant cross-flow. Conditions as in Fig. 7, except for L and τ = 5.0 min.

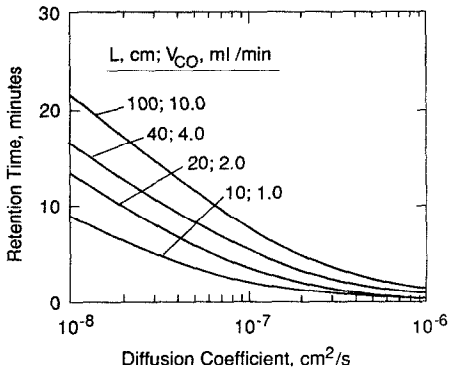

Fig. 13. Effect of channel length on retention in FlFFF with asymmetric channel using exponentially programmed force field: constant force field. Conditions as in Fig. 7, except for L, V_{co} and τ = 5.0 min.

mizes band-broadening difficulties that arise from utilizing some of the channel length at the inlet to contain the injected sample, as is often the case in sedimentation [15,21] and thermal [22,23] FFF separations.

However, the results are different if the initial force field is maintained constant by proportionately decreasing the cross-flow as the channel is shortened, as shown in Fig. 13. Here, decreasing the channel length with exponential programming also decreases retention. This situation may be more typical of actual experiments where the channel length is not usually changed as an operating parameter. The results in Fig. 13 suggest that channel lengths in the range 20–40 cm may be a good compromise for many FlFFF separations, whether constant-field or programmed-field operation is considered.

APPLICATIONS

Biological macromolecules

The ability to program the force field during the FlFFF separation allows the elution of a wide range of component sizes (molecular weight) to be eluted in a convenient time. This capability is illustrated in Fig. 14 by the 35-min separation of a synthetic mixture of proteins and plasmid DNAs (no time delay was used in the exponential decay program

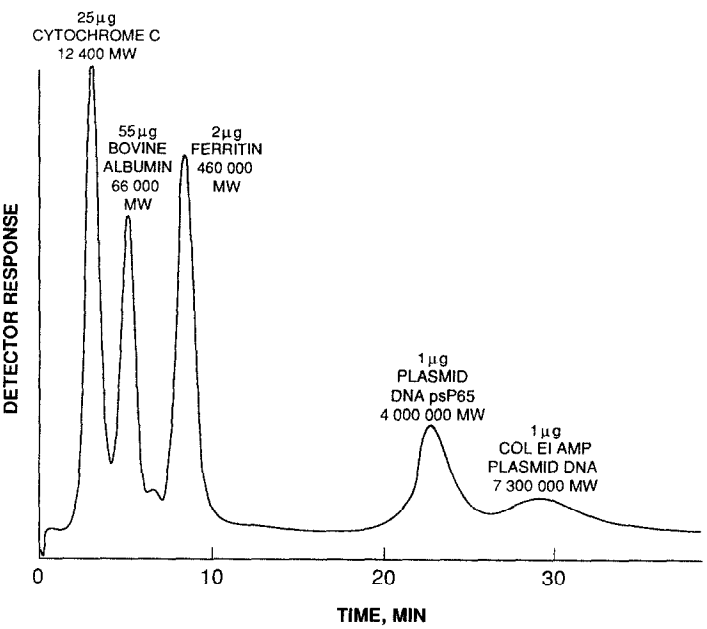

Fig. 14. Fractionation of proteins and nucleic acids with asymmetric channel using exponentially programmed force field. Channel, 41 × 2.0 × 0.0241 cm; focus distance, 4.3 cm; initial cross-flow, 9.0 ml/min; channel out-flow, 1.0 ml/min; sample injection at 0.06 ml/min for 4.0 min; sample injection/focus: pump (1) 1.0 ml/min, pump (2) 10.0 ml/min for a total of 8.0 min; exponential decay constant, 6.0 min; mobile phase, 0.05 *M* Tris buffer (pH 7.67)–0.05 *M* K_2SO_4–0.02% sodium azide; detector, UV, 260 nm, 0.02 a.u.f.s.; sample volume, 0.050 ml; components as shown.

used for this and the other applications reported in this paper). The first- and last-eluting compounds in the mixture in Fig. 14 have molecular weights of 12 400 and 7 300 000, respectively. This represents a molecular weight range ratio of about 600 separated in a single experiment. A stepwise gradient was previously used to separate human serum albumin from the dimer and trimer, but this approach involved a much narrower molecular weight range of components [13].

Calculation of the diffusion coefficients for the proteins in Fig. 14 produced values that closely correlated with those in the literature (*e.g.*, for cytochrome *c* and bovine serum albumin, $11.0 \cdot 10^{-7}$ and $5.8 \cdot 10^{-7}$ cm^2/s, respectively, compared with $11.1 \cdot 10^{-7}$ and $5.9 \cdot 10^{-7}$ cm^2/s reported [24]. However, values for the high-molecular-weight plasmids appeared to be considerably larger than those predicted, suggesting that these materials were retained additionally by some other mechanism. It appears unlikely that this additional retention was caused by chemical interaction with the membrane. This cellulosic membrane material normally does not display such effects, particularly in the pH–ionic strength environment used in this study. We speculate, therefore, that the added retention is due to physical interaction with micro-imperfections of the membrane surface. The strong initial force used for the separation probably pushes the large plasmids into observable micro-crevices or pockets in the membrane surface. Because of poor diffusion for these large components, significant time is required for diffusion out of the micro-crevices back into the normal channel flow streams. The net effect is that the components then elute at retention times that are larger than predicted. Apparently, more lightly retained components (such as the proteins in Fig. 14) do not interact deleteriously with the rough membrane surface, probably because they are not pushed sufficiently close to the surface by the particular crossed-flow force field used. These postulates are substantiated by constant force-field FlFFF separations with the same membrane (and membranes with similar surface-roughness properties) that elute components with predicted diffusion coefficients [6,7,13,14]. In these instances, modest force fields apparently did not push the components into a region in which the deleterious interaction with the membrane could occur.

The results with the large components in the separation in Fig. 14 and other similar experiments strongly suggest that much smoother membranes are needed for FlFFF. This is especially the case when programming with high initial force fields is used with samples containing large components. Studies to identify better membranes for FlFFF are in progress.

No attempt was made in Fig. 14 to optimize the range of component resolution or separation time. Therefore, all of these separation goals probably could be improved, if desired. Optimizing such a separation could be carried out by manipulating channel thickness, initial and outlet channel flow-rates and the value of the exponential time constant, τ. We believe that more than three decades of molecular weight difference can be comfortably spanned in a single FlFFF separation using optimized programming techniques.

Biological particulates

The use of exponential programming in FlFFF to separate a "real" sample of biological material is illustrated in Fig. 15. A 4-day-old isolate of *Streptococcus faecalis* bacteria was observed to have two minor and two major constituents. The minor components may be contaminating proteins that were expressed by the bacteria during storage at 4°C. The larger component eluting at *ca.* 21 min appears to be the "singles" or individual bacteria. The last large peak at *ca.* 30 min represents "chains" of these bacteria that are known to occur and are microscopically observed. Fig. 16 shows the particle-size (P_s) distributions associated with the two major peaks. These plots were obtained with software based on eqn. 3, using a special deconvolution method [25] to isolate each population effectively. The material in the first large peak eluting at 21 min demonstrated a weight-average diameter of 0.45 μm (Fig. 16A), with a sample polydispersity (weight-average/number-average) of 1.32 (uncorrected for band dispersion). This size is in keeping with microscopically observed values [26]. The differential plots in Fig. 16 relate the relative component concentration to the log (particle size) (P_s). The cumulative plot relates the relative weight fraction of the component to the log (particle size). The material in the second large peak at 30 min in Fig. 15 showed a weight-average diameter of 2.1 μm (Fig. 16B), with

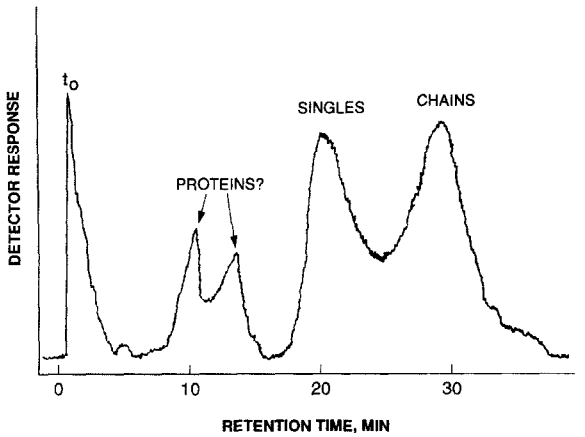

Fig. 15. Fractionation of *Streptococcus faecalis* bacteria sample with exponentially programmed FlFFF. Conditions as in Fig. 14, except initial cross-flow, 5.0 ml/min; channel out-flow, 2.0 ml/min; injection–focus, pump (1) 0.5 ml/min, pump (2) 4.5 ml/min for a total of 8.0 min; exponential decay time constant, 5.0 min; detector, 220 nm, 0.05 a.u.f.s.

a polydispersity of 1.52. These data suggest that this population is largely a mixture of 4–6-mer chains, with much smaller amounts of dimers largely in the "valley" between the two peaks. The data also suggest decreasing amounts of longer chains in the "tail" of the latter peak. Again, these results are in keeping with known properties associated with this bacterium and with microscopic observations [26].

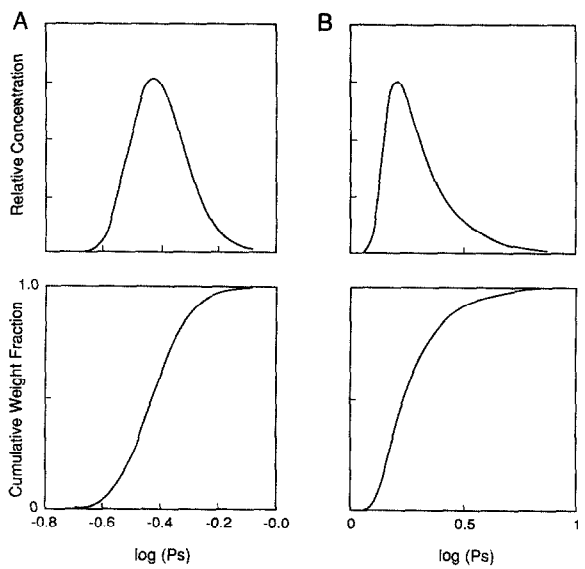

Fig. 16. Particle size distribution plots for *Streptococcus faecalis* bacteria. (A) 21-min peak (Fig. 15); (B) 30-min peak (Fig. 15). (A) Particle diameter: weight-average (A) 0.45 μm; (B) 2.1 μm; number-average: (A) 0.34 μm, (B) 1.4 μm; polydispersity: (A) 1.32, (B) 1.52.

The size of the "chains" in Fig. 15 might be expected to lead to earlier retention because of steric effects for these large components [27,28]. However, this effect apparently is not a strong feature under the conditions of force-field programming used. These and other of our studies in both FlFFF and SdFFF have suggested that force-field programming can be adapted to minimize steric effects associated with large components in mixtures of a wide size range. It is not intuitive that exponential programming actually minimizes the potential for steric interaction, if properly invoked. Smaller τ and V_{out} values reduce the tendency for steric interaction during an exponentially programmed separation. At the beginning of the separation, the initial high force field holds the components tightly so they essentially do not move down the channel; steric forces are inoperable. As the force field is decreased exponentially, the components rapidly move away from the accumulation wall, so that steric forces quickly become less effective.

Another phenomenon may have compensated for any steric effects that might have occurred in the separation in Fig. 15. Other studies in sedimentation FFF have shown that particle conformation can seriously affect retention. Components with high aspect ratios are apparently intercepted by faster flow streams than theoretical, causing earlier retention and smaller calculated particle sizes than expected [29].

Inorganic colloids

The utility of programmed FlFFF for measuring the particle-size distribution of inorganic colloids is shown in Fig. 17. This fractogram of a synthetic mixture containing three different silica sols of widely different sizes demonstrates the capability of the exponential programming method to analyze rapidly a sample of wide particle size distribution in a single experiment. A micro-mixing device was used between the channel and the detector to eliminate severe noise within the detector as the colloidal sample passed through the cell. This "noise" is caused by inhomogeneity in the channel effluent emerging from the channel. This effect can be

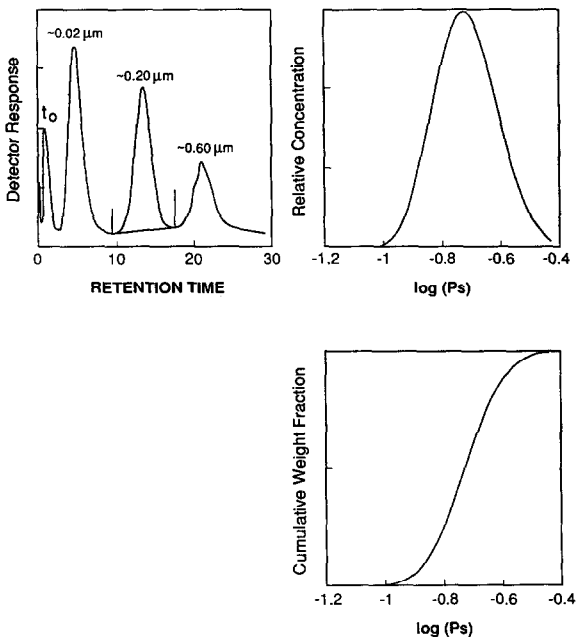

Fig. 17. Fractionation of silica sol mixture by exponentially programmed FlFFF. Conditions as in Fig. 14, except initial cross-flow, 3.0 ml/min; channel out-flow, 2.0 ml/min; injection–focus, pump (1) 0.3 ml/min, pump (2) 2.7 ml/min for a total of 5.0 min; exponential decay time constant, 4.0 min; sample, 0.050 ml of 2.5, 0.05 and 0.005% each of the increasingly larger silica sols; UV detector, 220 nm, 0.05 a.u.f.s. Particle diameter: weight-average 0.21 μm; number-average 0.18 μm; particle dispersity = 1.22. Retention time in min.

removed by using the stirring micro-mixer depicted in Fig. 1, or by using a low-volume packed-bed column of *ca.* 150-μm glass beads. Fig. 17 shows the differential and cumulative particle-size distribution plots of the middle-size component of this mixture, with a weight-average of 0.21 μm and a polydispersity of 1.22. Results for the 0.020- and 0.20-μm silica sols correlate closely with values obtained by sedimentation FFF for these samples. However, the calculated value for the 0.60-μm sample was significantly higher than that measured by transmission electron microscopy. This suggests an interaction of this material with the rough surface of the membrane in the same manner discussed for the plasmids in Fig. 14.

Synthetic polymers

FlFFF is well suited for characterizing a wide range of synthetic polymers, as illustrated by the separation of a commercial sample of polyacrylamide in Fig. 18. Fig. 18A is the detector signal obtained during the exponentially programmed separation. The values listed in the figure caption are various diffusion-coefficient averages and the sample polydispersity calculated for this sample. The smoothed differential and cumulative plots in Fig. 18B and C are the result of a computer deconvolution method used for the presentation.

The FlFFF method is not limited to water-soluble polymers. Organic-soluble polymers should be handled following minor alterations of our equipment. Future studies will investigate the proposed method for determining not only diffusion-coefficient distributions, but also molecular-weight distributions based on fundamental hydrodynamic volume relationships.

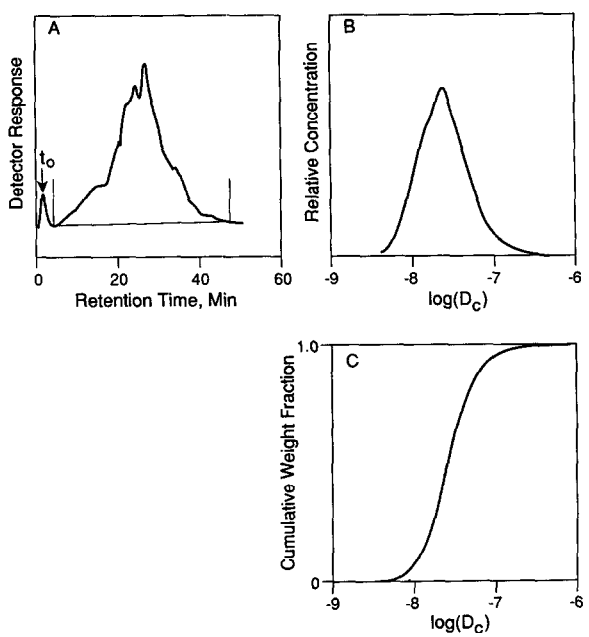

Fig. 18. FlFFF characterization of Sepran MLG polyacrylamide sample. Conditions as in Fig. 14, except mobile phase, 0.01 *M* KH_2PO_4 adjusted to pH 6.2 with NaOH; initial cross-flow, 5.0 ml/min; channel out-flow, 1.0 ml/min; exponential decay time constant, 7.0 min; sample 50 μl, 0.5% in mobile phase; detection, UV, 215 nm. $[D_c]_0 = 1.74 \cdot 10^{-8}$; $[D_c]_{+1} = 4.06 \cdot 10^{-8}$; $[D_c]_{+2} = 1.05 \cdot 10^{-7}$; $d_{[D_c]} = 2.33$.

CONCLUSIONS

This study has shown that exponentially programming the (cross-flow) force field in FlFFF is a convenient and effective way to provide data that permit the measurement of diffusion-coefficient- and particle-size-distributions of macromolecular components and particulates. Although an asymmetric rectangular channel was used as a model in this study, the described approach can be used for channels of any configuration. The method has certain distinct advantages over constant force-field operation, including (a) the ability to separate a wide range of components with a single experiment in a convenient time span; (b) maintaining more uniform resolution over a wide retention range; (c) easier detection of highly retained components; and (d) constant flow out the channel for constant detector response and good baseline stability. Although force-field programming involves more complicated apparatus, operation is simplified and made more reproducible with the use of automated computer-directed interfaces.

ACKNOWLEDGEMENTS

We thank V. Ivansons and E. R. Tinder, Jr., of the DuPont Experimental Station Engineering Crafts and Utilities Service Division for developing the computer-controlling system for the FlFFF instrument. We also thank R. C. Ebersole for the sample of *Streptococcus faecalis* bacteria.

APPENDIX

Derivation of eqns. 3 and 4

$$\chi = W$$

$$<\upsilon>_{in} \rightarrow \qquad\qquad \rightarrow <\upsilon>_{out}$$

$$\chi = 0 \qquad\qquad \downarrow \qquad\qquad \downarrow \qquad\qquad \downarrow$$

$$z = 0 \qquad\qquad u = \upsilon\chi \cdot \frac{W}{L} \qquad\qquad z = L$$

The migration of retained solutes moving downstream a distance z can be described as

$$\frac{dz}{dt} + \left(\frac{6D}{W^2}\right) z = \frac{6DL}{W^2}\left[\frac{<\upsilon>_{in}}{<\upsilon>_{in} - <\upsilon>_{out}}\right] \tag{A1}$$

Let $\upsilon_\chi = <\upsilon>_{in} - <\upsilon>_{out}$, then eqn. A1 becomes

$$\frac{dz}{dt} + \left(\frac{6D}{W^2}\right)z = \frac{6DL}{W^2}\left[\frac{\upsilon_\chi + <\upsilon>_{out}}{\upsilon_\chi}\right] = \frac{6DL}{W^2} + \frac{6DL}{W^2} \cdot \frac{<\upsilon>_{out}}{\upsilon_\chi}$$

or

$$\frac{dy}{dt} + \left(\frac{6D}{W^2}\right)y = -\left(\frac{6DL}{W^2}\right)\frac{<\upsilon>_{out}}{\upsilon_\chi} \tag{A2}$$

with $y = (L - z)$. The solution to the first-order ordinary differential equation of the type of eqn. A2 is readily available in the following form (with c = integration constant):

$$y = e^{\frac{-6Dt}{W^2}}\left\{c + \int e^{\frac{6Dt}{W^2}}\left[-\frac{6DL <\upsilon>_{out}}{W^2}\right]\frac{1}{\upsilon_\chi} \cdot dt\right\} \tag{A3}$$

Derivation of eqn. 3

For the case of exponential-decay force-field programming,

$$v_\chi = v_{\chi^\circ} e^{-t/\tau} \tag{A4}$$

and eqn. A3 becomes (with constant $\langle v \rangle_{out}$)

$$y = e^{\frac{-6Dt}{W^2}} \left\{ c + \int e^{\frac{6Dt}{W^2}} \left[- \frac{6DL \langle v \rangle_{out}}{v_{\chi^\circ} W^2} \right] e^{t/\tau} \, dt \right.$$

$$= c e^{\frac{-6Dt}{W^2}} - \frac{L \langle v \rangle_{out}}{v_{\chi^\circ}} \left(\frac{1}{1 + \frac{W^2}{6D\tau}} \right) e^{t/\tau} \tag{A5}$$

With the initial condition of $y = L - z$ at $t = 0$ (recalling that z is the sample focus distance in the channel), eqn. A5 gives the following expression for the integration constant c:

$$c = L - z + \frac{L \langle v \rangle_{out}}{v_{\chi^\circ}} \left(\frac{1}{1 + \frac{W^2}{6D\tau}} \right) \tag{A6}$$

At $t = t_R$, the solute emerges from the channel, when $z = L$ or $y = 0$. By combining eqns. A5 and A6 and setting $y = 0$:

$$\left[L - z + \frac{L \langle v \rangle_{out}}{v_{\chi^\circ}} \left(\frac{1}{1 + \frac{W^2}{6D\tau}} \right) \right] e^{\frac{-6Dt_R}{W^2}} = \left[\frac{L \langle v \rangle_{out}}{v_{\chi^\circ}} \left(\frac{1}{1 + \frac{W^2}{6D\tau}} \right) \right] e^{t_R/\tau} \tag{A7}$$

By rearranging and taking logarithms, eqn. A7 becomes

$$t_R = \frac{\tau}{1 + \frac{6D\tau}{W^2}} \cdot \ln \left[1 + \frac{L - z}{L} \cdot \frac{V_{co}}{V_{out}} \left(1 + \frac{W^2}{6D\tau} \right) \right] \tag{A8}$$

As $\langle v \rangle_{out} WB = v_{out}$ (volumetric flow-rate of channel effluent) and $u_o LG = V_{co}$ (initial volumetric cross-flow-rate),

$$\frac{V_{co}}{V_{out}} = \frac{U_o L}{\langle v \rangle_{out} W} = \frac{v_{\chi^\circ}}{\langle v \rangle_{out}} \tag{A9}$$

By substituting eqn. A9 in eqn. A8, we complete the derivation of eqn. 3:

$$t_R = \frac{\tau}{1 + \frac{6D\tau}{W^2}} \cdot \ln \left[1 + \frac{L - z}{L} \cdot \frac{V_{co}}{V_{out}} \left(1 + \frac{W^2}{6D\tau} \right) \right] \tag{A10}$$

Derivation of eqn. 4

For $t < \tau$, $v_\chi = v_{\chi^\circ}$, and for $t \geqslant \tau$, $v_\chi = v_{\chi^\circ} e^{-\frac{t-\tau}{\tau}}$. For $t < \tau$, from eqn. A3:

$$y = e^{-\frac{6Dt}{W^2}} \left\{ c + \int e^{\frac{6Dt}{W^2}} \left[- \frac{6DL \langle v \rangle_{out}}{v_{\chi^\circ} W^2} \right] dt \right\}$$

$$= c e^{\frac{-6Dt}{W^2}} - \frac{L \langle v \rangle_{out}}{v_{\chi^\circ}}$$

With the initial condition $y = L - z'$ at $t = 0$:

$$y_\tau = y_{t=\tau} = (L - z')\, e^{-\frac{6D\tau}{W^2}} + \frac{L <v>_{out}}{v_{\chi^o}}\left(e^{-\frac{6D\tau}{W^2}} - 1\right) \tag{A11}$$

For $t \geqslant \tau$, let $t' = t - \tau$ and from eqn. A3:

$$y = c'\, e^{-\frac{6Dt'}{W^2}} - \frac{6DL <v>_{out}}{v_{\chi^o} W^2} \cdot \frac{1}{\left(\frac{6D}{W^2}\right) + \frac{1}{\tau}} \cdot e^{t'/\tau} \tag{A12}$$

With the initial condition $y = y_\tau$ at $t' = 0$:

$$c' = y_\tau + \frac{L <v>_{out}}{v_{\chi^o}} \cdot \frac{1}{1 + \frac{W^2}{6D\tau}}$$

and

$$y = \left[(L - z')\, e^{-\frac{6D\tau}{W^2}} + \frac{L <v>_{out}}{v_{\chi^o}}\left(e^{-\frac{6D\tau}{W^2}} - 1 + \frac{1}{1 + \frac{W^2}{6D\tau}}\right)\right] e^{-\frac{6Dt'}{W^2}} - \frac{L <v>_{out}}{v_{\chi^o}}\left(\frac{1}{1 + \frac{W^2}{6D\tau}}\right) e^{t'/\tau} \tag{A13}$$

Since, at the time of solute elution, $t' = t_R - \tau$ at $y = 0$:

$$e^{\frac{t_R}{\tau}\left(1 + \frac{6D\tau}{W^2}\right)} = e \cdot \left\{\left(1 + \frac{W^2}{6D\tau}\right) \cdot \left[\frac{(L - z')\, v_{\chi^o}}{L <v>_{out}} + 1\right] - \frac{W^2}{6D\tau} e^{\frac{6D\tau}{W^2}}\right\} \tag{A14}$$

or

$$t_R = \left(\frac{\tau}{1 + \frac{6D\tau}{W^2}}\right)\left(1 + \ln\left\{1 + \left(\frac{L - z'}{L}\right)\frac{V_{co}}{V_{out}} + \frac{W^2}{6D\tau}\left[1 + \left(\frac{L - z'}{L} \cdot \frac{V_{co}}{V_{out}}\right) - e^{\frac{6D\tau}{W^2}}\right]\right\}\right)$$

$$= \left(\frac{\tau}{1 + \frac{6D\tau}{W^2}}\right)\left\{\left(1 + \frac{6D\tau}{W^2}\right) + \ln\left[\left(1 + \frac{L - z'}{L} \cdot \frac{V_{co}}{V_{out}}\right)\left(1 + \frac{W^2}{6D\tau}\right) e^{-\frac{6D\tau}{W^2}} - \frac{W^2}{6D\tau}\right]\right\}$$

And, finally we obtain eqn. 4:

$$t_R = \tau + \left(\frac{\tau}{1 + \frac{6D\tau}{W^2}}\right) \ln\left\{1 + \left[\left(\frac{L - z'}{L} \cdot \frac{V_{co}}{V_{out}}\right)\left(1 + \frac{W^2}{6D\tau}\right)\right] + \left[\frac{W^2}{6D\tau}\left(e^{-\frac{6D\tau}{W^2}} - 1\right)\right]\right\} \tag{A15}$$

REFERENCES

1 J. C. Giddings, *Sep. Sci.*, 1 (1966) 123.
2 E. Grushka, K. D. Caldwell, M. N. Myers and J. C. Giddings, in E. S. Perry, C. J. Van Oss and E. Grushka (Editors), *Separation and Purification Methods*, Vol. 2, Marcel Dekker, New York, 1973, p. 127.
3 J. C. Giddings, *J. Chem. Educ.*, 50 (1973) 667.
4 J. C. Giddings, M. N. Myers, K. D. Caldwell and S. R. Fisher, *Methods Biochem. Anal.*, 26 (1980) 79.
5 K. D. Caldwell, *Anal. Chem.*, 60 (1988) 959A.
6 K.-G. Wahlund and J. C. Giddings, *Anal. Chem.*, 59 (1987) 1332.
7 K.-G. Wahlund and A. Litzen, *J. Chromatogr.*, 461 (1989) 73.
8 J. C. Giddings, F. J. Yang and M. N. Myers, *Anal. Chem.*, 48 (1976).

9 J. C. Giddings, G. C. Lin and M. N. Myers, *J. Colloid Interface Sci.*, 65 (1978) 67.
10 J. J. Kirkland, C. H. Dilks, Jr. and W. W. Yau, *J. Chromatogr.*, 255 (1983) 255.
11 K.-G. Wahlund, H. S. Winegarner, K. D. Caldwell and J. C. Giddings, *Anal. Chem.*, 58 (1986) 573.
12 J. A. Jönsson and A. Carlshaf, *Anal. Chem.*, 61 (1989) 11.
13 A. Litzen and K.-G. Wahlund, *J. Chromatogr.*, 476 (1989) 413.
14 A. Litzen and K.-G. Wahlund, poster presented at the *International Symposium on Polymer Analysis and Characterization*, Brno, July 23–25, 1990.
15 J. J. Kirkland, W. W. Yau, W. A. Doerner and J. W. Grant, *Anal. Chem.*, 52 (1980) 1944.
16 W. W. Yau and J. J. Kirkland, *Sep. Sci. Technol.*, 16 (1981) 577.
17 J. J. Kirkland and W. W. Yau, *US Pat.*, 4 285 810 (1981).
18 J. J. Kirkland and W. W. Yau, *Macromolecules*, 18 (1985) 2305.
19 J. J. Kirkland, S. W. Rementer and W. W. Yau, *Anal. Chem.*, 60 (1988) 610.
20 S. Glasstone, *Textbook of Physical Chemistry*, Van Nostrand, New York, 2nd ed., 1946, p. 260.
21 C. H. Dilks, Jr., W. W. Yau and J. J. Kirkland, *J. Chromatogr.*, 315 (1984) 45.
22 J. C. Giddings, S. Li, P. S. Williams and M. E. Schimpf, *Makromol. Chem., Rapid Commun.*, 9 (1988) 817.
23 J. C. Giddings, L. K. Smith and M. N. Myers, *Anal. Chem.*, 48 (1976) 1587.
24 H. A. Sober (Editor), *Handbook of Biochemistry*, Chemical Rubber Co., Cleveland, OH, 2nd ed., 1970, Section C.
25 S. W. Rementer, Experimental Station, DuPont, Wilmington, DE, unpublished studies, 1991.
26 R. C. Ebersole, Experimental Station, DuPont, Wilmington, DE, unpublished studies, 1990.
27 M. N. Myers and J. C. Giddings, *Anal. Chem.*, 54 (1982) 2284.
28 S. Lee and J. C. Giddings, *Anal. Chem.*, 60 (1988) 2328.
29 J. J. Kirkland, L. E. Schallinger and W. W. Yau, *Anal. Chem.*, 57 (1985) 2271.